ELSEVIER

Catalysis Today 32 (1996) 47–55

CATALYSIS TODAY

In situ Raman spectroscopy studies of bulk and surface metal oxide phases during oxidation reactions

Israel E. Wachs [a], Jih-Mirn Jehng [a,1], Goutam Deo [a], Bert M. Weckhuysen [a,2], Vadim V. Guliants [b,3], Jay B. Benziger [b,*]

[a] *Zettlemoyer Center for Surface Studies, Department of Chemical Engineering, Lehigh University, Bethlehem, PA 18015, USA*
[b] *Princeton Material Institute, Princeton University, NJ 08544, USA*

Abstract

Bulk V-P-O and model supported vanadia catalysts were investigated with in situ Raman spectroscopy during *n*-butane oxidation to maleic anhydride in order to determine the fundamental molecular structure–reactivity/selectivity insights that can be obtained from such experiments. The in situ Raman studies of the bulk V-P-O catalysts provided information about the bulk crystalline phases, the hemihydrate precursor and its transformation to vanadyl pyrophosphate. However, the Raman experiments could not provide any molecular structural information about the amorphous and surface phases also present in this bulk metal oxide catalyst because of the strong Raman scattering from the crystalline phases. In contrast, in situ Raman studies of the model supported vanadia catalysts, where the active phase is present as a two-dimensional surface metal oxide overlayer, provided new insights into this important hydrocarbon oxidation reaction. In addition, the surface properties of the supported vanadia catalysts could be molecularly engineered to probe the role of various functionalities upon the structure–reactivity/selectivity relationship of *n*-butane oxidation to maleic anhydride. These fundamental studies revealed that the oxidation of *n*-butane required only one surface vanadia site and that the critical rate determining step involved the bridging V–O–P or V–O-support bonds. The selective oxidation of *n*-butane to maleic anhydride could occur over one surface vanadia site as well as multiple adjacent surface vanadia sites, but the reaction is more efficient with multiple sites. The *n*-butane oxidation TOF increased with the introduction of both surface Brönsted and Lewis acid sites, but only the surface Lewis acid sites increased the maleic anhydride selectivity.

Keywords: Raman spectroscopy; Bulk metal oxide phase; Surface metal oxide phase; Oxidation reactions; Metal oxide

1. Introduction

Metal oxide catalysts are extensively employed for selective oxidation reactions in the petrochemical, energy and pollution control industries [1]. Bulk metal oxide catalysts, where the active phase is distributed throughout the entire catalyst, selectively oxidize propylene and ammonia to acrylonitrile (Bi-Mo-O), propane and ammonia to acrylonitrile (V-Sb-O), benzene

* Corresponding author.

[1] Present address: Department of Chemical Engineering, National Chung-Hsing University, Taichung 402, Taiwan, RO China.

[2] Present address: Centrum voor Oppervlaktechemie en Katalyse, K.U. Leuven, Kardinaal Mercierlaan 92, B-3001 Heverlee, Belgium.

[3] Present address: Praxair, Inc., 175 East Park Drive, P.O. Box, Tonawanda, NY 14151, USA.

PII S0920-5861(96)00091-0

to maleic anhydride (V-Mo-O), *n*-butane to maleic anhydride (V-P-O), *n*-pentane to maleic/phthalic anhydride (V-P-O) and methanol to formaldehyde (Fe-Mo-O) [2]. Supported metal oxide catalysts, where the active phase is present as a two-dimensional surface metal oxide overlayer on the oxide support, selectively oxidize *o*-xylene to phthalic anhydride (V_2O_5/TiO_2), aromatic methyl groups with ammonia to nitrile groups (V_2O_5/TiO_2), chlorinated hydrocarbons to CO_2 and HCl (CrO_3/Al_2O_3) and selectively reduce NOx with ammonia to N_2 (V_2O_5-WO_3/TiO_2 and V_2O_5-MoO_3-WO_3/TiO_2) [3]. The widespread use of metal oxide catalysts in industry has initiated many fundamental studies into their molecular structure–reactivity/selectivity relationships [4,5]. Raman spectroscopy is one of the few characterization techniques that can provide fundamental molecular structural information about metal oxide catalysts during oxidation reactions [5–9]. The type of fundamental information that can be obtained with in situ Raman spectroscopy studies of metal oxide catalysts will be examined in this paper. The present study will focus on the selective oxidation of *n*-butane to maleic anhydride over bulk V-P-O and model supported vanadia catalysts in order to contrast the different information that can be obtained about bulk and surface metal oxide phases from in situ Raman spectroscopy studies.

2. Experimental

The preparation of the bulk V-P-O catalysts has been described in detail elsewhere [10]. The model supported vanadia catalysts were prepared by the incipient-wetness impregnation method [11] using the following metal oxide supports: TiO_2 (Degussa, ~ 55 m^2/g), ZrO_2 (Degussa, ~ 39 m^2/g), Nb_2O_5 (Niobium Products Company, ~ 50 m^2/g), CeO_2 (~ 36 m^2/g), Al_2O_3 (Harshaw, ~ 180 m^2/g) and SiO_2 (Cab-O-Sil, EH-5, ~ 380 m^2/g).

A detailed description of the in situ Raman spectrometer system may be found elsewhere [11].

The microreactor employed in the kinetic studies as well as the gas chromatographic analysis of the catalytic reaction products have been described in detail in our previous publication [10].

3. Results and discussion

For bulk metal oxide catalysts, Raman spectroscopy provides information about the bulk sites since it is inherently a bulk spectroscopy (typically about 1 micron depth analysis) [6–8,12]. Consequently, insights can be obtained about (1) the structure of bulk crystalline metal oxide phases, (2) the extent of crystallization of bulk metal oxide phases, (3) the phase transformations of bulk metal oxide phases, (4) the coordination of bulk metal oxide sites and (5) the participation of specific metal oxide bonds in catalysis (with the aid of oxygen-18 isotopic tracer studies). Unfortunately, information about the surface of the bulk metal oxide catalysts can not be obtained because of the significantly stronger Raman scattering from the crystalline bulk metal oxide phases (typically orders of magnitude greater). Coexisting amorphous phases similarly can not be detected because of their much weaker Raman scattering relative to crystalline bulk metal oxide phases, but amorphous phases may be detectable in the absence of accompanying crystalline bulk metal oxide phases. Thus, Raman spectroscopy primarily provides structural information about the crystalline phases present in bulk metal oxide catalysts.

As an example of a bulk metal oxide catalyst system, the oxidation of *n*-butane to maleic anhydride over a V-P-O catalyst will be examined with in situ Raman spectroscopy. The commercial V-P-O catalyst employed for *n*-butane oxidation to maleic anhydride is initially synthesized as a hemihydrate precursor, $VOHPO_4 \cdot 0.5H_2O$, and is subsequently transformed to the

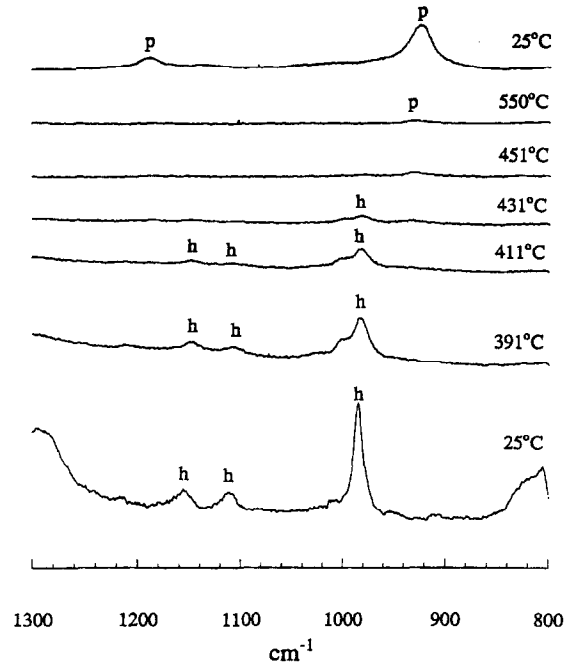

Fig. 1. In situ Raman of transformation of the $VOHPO_4 \cdot 0.5H_2O$ precursor to vanadyl pyrophosphate in helium.

active vanadyl pyrophosphate phase, $(VO)_2P_2O_7$, [13,14]. The transformation of the hemihydrate precursor to the active pyrophosphate phase in a helium atmosphere was monitored via in situ Raman spectroscopy as a function of temperature as shown in Fig. 1. The hemihydrate precursor possesses several Raman bands in the 900–1000 cm^{-1} region which are labelled h. Heating the hemihydrate precursor to approximately 400°C results in a decrease of the Raman hemihydrate signal due to thermal broadening and decomposition of this phase. The hemihydrate Raman signal is essentially absent above 431°C due to its complete transformation, but a corresponding Raman signal for the pyrophosphate phase is not observed until the sample is cooled to room temperature (Raman peaks are labelled p). The absence of a strong pyrophosphate signal at elevated temperatures reveals that the pyrophosphate phase is initially not well crystallized and may also possess an amorphous component. This is confirmed by the further crystallization of the pyrophosphate phase, about a factor of 5 increase in Raman intensity, during the initial 20–30 days of *n*-butane oxidation and the direct observation of an amorphous layer on the (200) planes of the vanadyl pyrophosphate crystals with high resolution-transmission electron microscopy (HR-TEM) [10]. The HR-TEM studies reveal that the amorphous layer, initially ~ 1.5 nm thick, contracts and completely disappears within 23 days of *n*-butane oxidation. The crystallization of the vanadyl pyrophosphate surface coincided with a much higher steady state selectivity to maleic anhydride (the selectivity increased from 47 to 62% at 25% conversion of *n*-butane). During this period, the transformed catalyst only exhibited the Raman features of vanadyl pyrophosphate and no additional Raman bands were observed during in situ Raman studies of *n*-butane oxidation over the catalyst. The presence of an amorphous phase during the transformation of the hemihydrate precursor to the active vanadyl pyrophosphate phase has also recently been concluded in publications by Cavani and Trifirò [13] and Hutchings et al. [14].

The above studies demonstrate that Raman spectroscopy provided bulk information about the V-P-O catalysts (crystalline phases present, phase transformation and extent of crystallization), but could not provide direct information about the amorphous phase or the surface of this catalyst. The corresponding catalytic data revealed that the crystallization of the amorphous layer on the (200) planes of the vanadyl pyrophosphate crystals was critical for the enhanced selectivity towards maleic anhydride. Thus, Raman spectroscopy is not able to provide the fundamental molecular structural information about the catalyst surface as well as the amorphous phase for this bulk oxide system because of its greater sensitivity towards the crystalline bulk V-P-O phases. Unfortunately, other molecular spectroscopies (NMR, EXAFS/XANES, UV-Vis DRS and IR) are also not able to provide information about the molecular structure of the surface present in V-P-O catalysts because of their much stronger signals from the

catalyst bulk than the catalyst surface [15]. Limitations of both bulk and surface characterization techniques currently available, coupled with the complex solid-state chemistry of vanadium phosphates, have led to considerable confusion and contradictions in the literature concerning the identity of the active sites involved in different steps of *n*-butane oxidation to maleic anhydride over V-P-O catalysts [15].

Unlike bulk metal oxide catalysts, detailed surface structural information on a molecular level can be obtained from model supported metal oxide catalysts containing two-dimensional overlayers of surface metal oxide species [3,6–9]. A unique feature of supported metal oxide catalysts is that the active component is exclusively present as a dispersed phase, 100% dispersion, below monolayer coverage and there are no spectroscopic complications from the coexistence of bulk crystalline phases. The only bulk crystalline phases present below monolayer coverage are due to the oxide supports (titania, zirconia, etc.), but these oxides typically give rise to weak Raman signals that usually occur at much lower frequencies than the active surface metal oxide species. For supported vanadia catalysts [16], Raman spectroscopy provides direct fundamental surface information about (1) the ratio of isolated and polymerized surface vanadia species, (2) terminal V = O and bridging V–O–V bonds, (3) extent of reduction of the surface vanadia species during catalysis, (4) influence of the oxide support ligands, (5) influence of acidic/basic metal oxide additives (promoters/poisons) and participation of specific M–O bonds in catalysis (with the aid of oxygen-18 labelled isotope experiments). The Raman studies, however, can not provide direct information about the V–O-support bonds because they are slightly ionic and, consequently, Raman inactive [9]. Thus, in situ Raman studies during oxidation reactions over model supported metal oxide catalysts can provide new insights into the surface properties of oxide catalysts which are not attainable with bulk metal oxide catalysts.

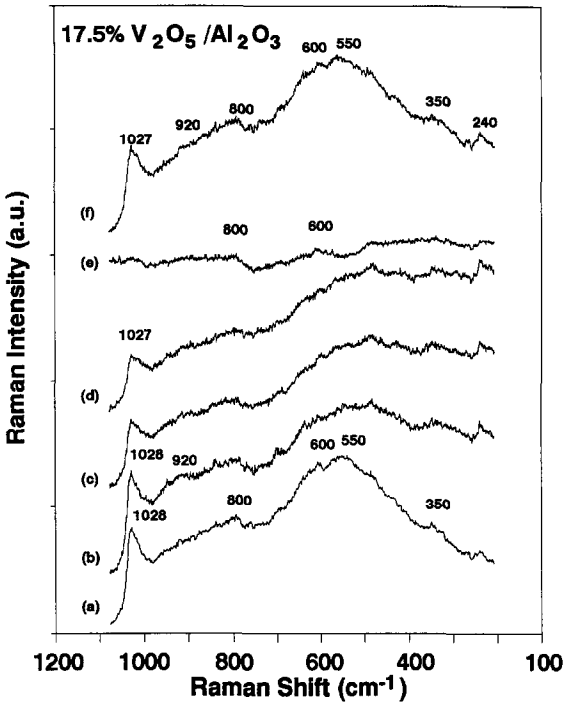

Fig. 2. In situ Raman of *n*-butane oxidation over 17.5% V_2O_5/Al_2O_3 catalyst: (a) O_2, 100 cc/min, 230°C; (b) C_4H_{10}/O_2/He, 100 cc/min, 230°C; (c) C_4H_{10}/O_2/He, 100 cc/min, 300°C; (d) C_4H_{10}/O_2/He, 100 cc/min, 350°C; (e) C_4H_{10}/He, 100 cc/min, 350°C; (f) O_2, 350°C.

The oxidation of *n*-butane to maleic anhydride over model supported vanadia catalysts was investigated with in situ Raman spectroscopy in order to obtain additional fundamental insights into this important catalytic reaction. The model supported metal oxide catalysts consisted of (1) surface vanadia phases on different oxide supports approaching monolayer coverage, (2) surface vanadia species on TiO_2 as a function of surface coverage and (3) surface vanadia and surface phosphate species on TiO_2. The in situ Raman spectra of a 17.5% V_2O_5/Al_2O_3 catalyst (approximately 90% of monolayer coverage) during *n*-butane oxidation are presented in Fig. 2. The fully oxidized catalyst exhibited Raman bands at 920, 800, 600 and 550 cm^{-1} due to the presence of bridging V–O–V bonds and 1028 cm^{-1} due to terminal V = O bonds. During *n*-butane oxidation, the polymeric bridging V–O–V functionalities be-

Table 1
The effect of the metal oxide support on *n*-butane oxidation on supported vanadia catalysts at 221°C in 1.2 vol% *n*-butane in air

Catalyst	Weight (g)	Flow (cc/min)	Butane conversion (mol%)	MA [a] selectivity (mol%)	Butane TOF (10^{-5} s^{-1})	MA TOF (10^{-5} s^{-1})
$7\%V_2O_5/SiO_2$	0.577	7.4	< 2	Tr	0.4	Tr
[b]		11.9	28.6	16.6	6.0	1.0
$17.5\%V_2O_5/Al_2O_3$	0.625	17.8	7.2	44.5	0.9	0.4
$6\%V_2O_5/Nb_2O_5$	0.885	13.9	17.3	36.7	3.6	1.3
$4\%V_2O_5/ZrO_2$	0.794	11.3	16.0	9.3	4.5	0.4
$3\%V_2O_5/CeO_2$	0.622	14.2	10.6	12.6	6.3	0.8
$5\%V_2O_5/TiO_2$	0.566	25.5	27.8	30.5	19.6	6.0

[a] MA = maleic anhydride.
[b] The data in this row were collected at 350°C.

came more extensively reduced than the terminal V = O bonds (compare Fig. 2a and Fig. 2b–d). At higher temperatures, the reduction of the terminal V = O bond became more pronounced (compare Fig. 2a and Fig. 2d). In the absence of oxygen, both the terminal V = O and bridging V–O–V bonds were essentially absent from the Raman spectrum due to extensive reduction of these functionalities (see Fig. 2e). Unfortunately, the reduced surface vanadia species did not give rise to new Raman bands because of their weak or inactive Raman signals. Exposure to an oxygen environment readily reoxidized the surface vanadia species and yielded the initial Raman spectrum (compare Fig. 2a and Fig. 2f). Essentially the same trends were observed with other supported vanadia catalysts (vanadia/titania, vanadia/zirconia, vanadia/niobia, and vanadia/ceria): the surface vanadia species were partially reduced during *n*-butane oxidation and the polymeric bridging V–O–V functionality was always more extensively reduced than the terminal V = O bond functionality. For the V_2O_5/SiO_2 catalyst, however, the polymeric V–O–V functionality was absent and the terminal V = O bond was not reduced during *n*-butane oxidation. Thus, the general observation is that the surface vanadia (+5) species are only partially reduced during *n*-butane oxidation and that the polymeric bridging V–O–V functionality is more extensively reduced than the terminal V = O functionality.

The performance of the supported vanadia catalyst during *n*-butane oxidation is shown in Table 1 as a function of the specific oxide support. The butane turnover frequency (TOF), the number of butane molecules converted per surface vanadia species per second, reveals that the TOF is a strong function of the specific oxide support and varies by a factor of approximately 50 (titania > ceria > zirconia > niobia > alumina > silica). Comparison of the butane oxidation TOF with the corresponding extent of reduction of the surface vanadia species during

Table 2
Performance of titania support in *n*-butane oxidation at 221°C in 1.2 vol% *n*-butane in air

Catalyst	Weight (g)	Flow (cc/min)	Butane conversion (mol%)	MA selectivity (mol%)	Butane TOF (10^{-5} s^{-1})	MA TOF (10^{-5} s^{-1})
$1\%V_2O_5/TiO_2$	0.890	8.7	16.0	22.8	12.4	2.8
$2\%V_2O_5/TiO_2$	0.612	17.6	24.2	9.9	27.7	2.7
$3\%V_2O_5/TiO_2$	0.603	19.9	27.0	17.0	23.4	4.0
$4\%V_2O_5/TiO_2$	0.700	30.7	30.7	29.9	25.5	6.6
$5\%V_2O_5/TiO_2$	0.566	25.5	27.8	30.5	19.6	6.0

the in situ Raman studies demonstrates that there is no correlation between these two parameters. For example, during *n*-butane oxidation the most extensively reduced supported vanadia catalyst was vanadia/alumina and the least reduced supported vanadia catalyst was vanadia/silica, but these were the two least active catalyst systems for this oxidation reaction. The butane TOF was also found not to be strongly dependent on the surface vanadia coverage for the vanadia/titania catalyst system (see Table 2). This observation suggests that (1) the *n*-butane oxidation TOF is not related to the concentration of polymeric bridging V–O–V functionality, which increases with surface vanadia coverage for this system [17,18] and (2) that butane oxidation, the sum of the selective and nonselective oxidation reactions, requires primarily one surface vanadia site [9,16]. The *n*-butane oxidation TOF also did not correlate with the Raman band position, or bond strength, of the terminal V = O bond which was approximately the same during *n*-butane oxidation, 1025–1028 cm^{-1}, for vanadia/titania, vanadia/zirconia and vanadia/alumina, but the corresponding *n*-butane oxidation TOF varied by approximately a factor of 20. In situ Raman experiments with oxygen-18 labelling of the terminal V = O bond during butane oxidation showed that the exchange time of this bond was approximately 20 times longer than the characteristic reaction time (1/TOF), and suggests that this bond is too stable to be involved with the rate determining step of this reaction. The strong influence of the specific oxide support ligand on the *n*-butane oxidation TOF, approximately a factor of 50, suggests that the bridging V–O-support bonds are involved in the critical rate determining step associated with *n*-butane oxidation.

The maleic anhydride selectivities for the various supported vanadia catalysts containing high surface coverages are shown in Table 1. The maleic anhydride selectivity trend varied as follows: alumina > niobia > titania > zirconia > ceria. This trend parallels the strength of the Lewis acid sites of the oxide supports: alumina > niobia > titania ~ zirconia [19]. This observation is consistent with the critical reaction step involving the bridging V–O-support bond which is in immediate vicinity of the Lewis acid sites of the oxide support. The influence of surface vanadia coverage on the titania support upon the maleic anhydride selectivity is presented in Table 2. With the exception of the lowest vanadia coverage, the maleic anhydride selectivity increases with surface vanadia coverage up to monolayer coverage (~ 6% V_2O_5/TiO_2). At the higher coverages, a maleic anhydride selectivity of approximately 30% is obtained at approximately 30% conversion of *n*-butane. A similar increasing trend with surface vanadia coverage is seen for the maleic anhydride TOF in Table 2. The increasing maleic anhydride selectivity and TOF with surface vanadia coverage suggests that adjacent surface vanadia sites, possibly two sites, are more efficient in selectively oxidizing *n*-butane to maleic anhydride than the isolated surface vanadia sites which predominate at lower surface vanadia coverages. However, the results also suggest that isolated surface vanadia sites are capable of oxidizing *n*-butane to maleic anhydride since such sites predominate at low surface vanadia coverages [16–18]. This is further confirmed by the butane oxidation studies over the vanadia/silica catalyst where only isolated surface vanadia sites are present and maleic anhydride production is also observed at elevated temperatures (see Table 1). Thus, the selective oxidation of butane to maleic anhydride can occur over isolated as well as multiple adjacent surface vanadia sites, but the process is more efficient with adjacent surface vanadia sites.

The influence of surface phosphate species on the 1% V_2O_5/TiO_2 catalyst was also examined with in situ Raman spectroscopy and *n*-butane oxidation. The surface phosphate species were anchored to the titania support prior to the introduction of the surface vanadia species. The surface phosphate species on titania have been found to possess a tridentate hydrogenphosphate

structure, HO-P(-O-Ti)$_3$, with weak Brönsted acid sites [21]. The subsequent introduction of surface vanadia species is expected to form V–O–P bonds via titration of the POH bonds of the surface phosphate species as well as some V–O–Ti bonds to exposed Ti–OH sites [9,16,21]. The in situ Raman studies demonstrated that this two-step preparation procedure results in the formation of surface vanadia species coordinated to the phosphated titania support (no crystalline V-P-O phases are formed [20]) and that the surface vanadia species remain essentially fully oxidized during *n*-butane oxidation. The corresponding catalytic performance of the 1% V_2O_5/5% P_2O_5/TiO_2 and the unpromoted 1% V_2O_5/TiO_2 catalysts are presented in Table 3. The surface phosphate promoter increased both the *n*-butane oxidation TOF and the maleic anhydride selectivity by more than a factor of 2 at comparable conversions of *n*-butane oxidation. A maleic anhydride selectivity of 56% was obtained at 12.1% butane conversion. This combined increase in *n*-butane oxidation and maleic anhydride selectivity resulted in more than a factor of 5 increase in the maleic anhydride TOF. This dramatic increase in the maleic anhydride production demonstrates the importance of bridging V–O–P bonds during *n*-butane oxidation to maleic anhydride. This observation is consistent with the above conclusion that the bridging V–O-support bond is involved in the critical step during *n*-butane oxidation.

The influence of surface Brönsted acid and Lewis acid sites on the behavior of a 1% V_2O_5/TiO_2 were also examined by introducing surface tungsten oxide and surface niobium oxide species, respectively [19,20]. In situ Raman studies revealed that the tungsten oxide and niobia additives was present on the titania surface as two-dimensional surface metal oxide species (no bulk oxide phases and no complexes with the surface vanadia species). The influence of these two surface metal oxide additives on the performance of the 1% V_2O_5/TiO_2 catalyst during *n*-butane oxidation are presented in Table 3. The introduction of the surface tungsten oxide Brönsted acid sites increased the surface butane oxidation TOF by almost a factor of 3, but did not appear to have a significant influence on the maleic anhydride selectivity. The higher *n*-butane oxidation TOF was responsible for the higher maleic anhydride TOF since the maleic anhydride selectivity was almost unchanged by the surface tungsten oxide additive. In contrast, the introduction of the surface niobia Lewis acid sites increased the *n*-butane oxidation TOF by a factor of more than 4 and also had approximately a 50% improvement in maleic anhydride selectivity. The combined increase in *n*-butane oxidation TOF and maleic anhydride selectivity resulted in more than a factor of 6 increase in the maleic anhydride TOF due to the introduction of the surface niobia additive. Thus, both surface Brönsted acid and Lewis acid sites improve the performance of *n*-butane oxidation to maleic anhydride, but the Brönsted acid sites appear to only increase the oxidation of *n*-butane while the Lewis acid sites increase both the oxidation of *n*-butane and the maleic anhydride selectivity.

The above fundamental studies with in situ Raman and *n*-butane oxidation involving the model supported vanadia catalysts provide new

Table 3
The effect of acidic promoters on *n*-butane oxidation on the 1%V_2O_5/TiO_2 catalyst at 221°C in 1.2 vol% *n*-butane in air

Catalyst	Weight (g)	Flow (cc/min)	Butane conversion (mol%)	MA selectivity (mol%)	Butane TOF (10^{-5} s^{-1})	MA TOF (10^{-5} s^{-1})
1%V_2O_5/TiO_2	0.890	8.7	16.0	22.8	12.4	2.8
1%V_2O_5/5%P_2O_5/TiO_2	0.172	5.0	12.1	56.2	27.0	15.2
6%WO_3/1%V_2O_5/TiO_2	0.708	8.9	23.6	26.2	34.1	8.9
6%Nb_2O_5/1%V_2O_5/TiO_2	0.181	7.5	10.7	35.1	50.8	17.8

surface molecular information about this important hydrocarbon oxidation reaction. Such fundamental insights were not directly achievable with corresponding in situ Raman studies of bulk V-P-O catalysts because of the limitations of the Raman characterization technique with regard to providing surface molecular information about bulk metal oxide catalysts. According to the bulk V-P-O catalyst literature, experimental results support the conclusions that the best catalysts preferentially expose the (200) planes of $(VO)_2P_2O_7$, and that the bulk vanadyl pyrophosphates serves as a support for this active surface [13,15]. The recent models for *n*-butane oxidation are based on the presence of vanadyl dimers in the (200) plane of vanadyl pyrophosphate [13,15]. The following types of hypothetical active sites have been proposed to exist on the active (200) plane of bulk vanadyl pyrophosphate catalysts: (1) Brönsted acid sites, (2) Lewis acid sites, (3) one electron redox couple: V^{4+}/V^{5+} and V^{3+}/V^{4+}, (4) two electron redox couple: V^{3+}/V^{5+}, (5) bridging oxygen (V–O–V and V–O–P), (6) terminal oxygen (V = O) and (7) activated molecular oxygen: peroxo and superoxo species [13]. The current studies with the model supported vanadia catalysts are in agreement with the important roles of Brönsted and Lewis acid sites, but Lewis acid sites appear to have a more pronounced effect on the maleic anhydride selectivity than the surface Brönsted acid sites. The bridging oxygen, V–O–P or V–O-support, is the critical bond that controls the rate determining step for the selective oxidation of *n*-butane to maleic anhydride. The terminal V = O and polymeric bridging V–O–V bonds, however, do not appear to influence the *n*-butane oxidation TOF or maleic anhydride selectivity. Furthermore, the oxidation state of the surface vanadia species does not appear to correlate with either the activity or selectivity of *n*-butane oxidation to maleic anhydride. It is not possible to determine from the present in situ Raman studies if a one electron or two electron redox couple is operating during *n*-butane oxidation over these model supported vanadia catalysts because the reduced surface vanadia species, V^{4+} and V^{3+}, do not give rise to a detectable Raman signal. Such information should be readily obtainable from an in situ DRS UV-Vis investigation with the model supported vanadia catalysts and such studies are currently in progress [22]. The model supported vanadia catalytic studies also revealed that only one surface vanadia site is required for the oxidation of *n*-butane and that maleic anhydride can be produced with only one surface vanadia site. However, the production of maleic anhydride is more efficient with multiple adjacent surface vanadia sites or surface vanadia dimers. Activated adsorbed molecular oxygen species, peroxo and superoxo, are Raman active, but such signals were not detected in any of the in situ Raman experiments (especially with the vanadia/phosphate/titania catalyst which exhibited a relatively high maleic anhydride selectivity).

4. Conclusions

Bulk V-P-O and model surface vanadium oxide catalysts were investigated during *n*-butane oxidation to maleic anhydride with in situ Raman spectroscopy. The Raman studies with the bulk V-P-O catalyst provided structural information about the transformation of the hemihydrate precursor to the active vanadyl pyrophosphate phase, but could not provide any information about the nature of the amorphous and surface phases present in such bulk metal oxide catalysts. Consequently, it was not possible to establish surface molecular structure–reactivity relationships for the bulk V-P-O catalyst.

In contrast, it was possible to directly monitor the surface phases present in model supported vanadia catalysts, which contain the active surface vanadia phase as a two-dimensional overlayer (100% dispersed), with Raman spectroscopy. In addition, it was also possible to molecularly engineer the different surface sites

present in such model supported vanadia catalysts: ratio of isolated to polymerized surface vanadia species, the presence of bridging V–O–P bonds, the presence of surface Brönsted acid and Lewis acid sites, and the nature of bridging V–O-support bonds. Combination of the Raman surface molecular structural information, design of the nature of the surface metal oxide sites, and *n*-butane oxidation studies allowed the development of fundamental surface molecular structure–reactivity relationships for this important hydrocarbon oxidation reaction.

Acknowledgements

The work at Lehigh University was supported by the Division of Basic Energy Sciences, Department of Energy under grant DEFG02-93ER14350. V.V.G. and J.B.B. wish to thank the AMOCO Chemical Corporation and National Science Foundation (grant CTS-9100130) for support. B.M.W. wishes to acknowledge the 'Belgisch Nationaal Fonds voor Wetenschappelijk Onderzoek' for a travel grant.

References

[1] C.L. Thomas, Catalytic Processes and Proven Catalysts, Academic Press, New York, 1970.
[2] J. Brazdil, in I.E. Wachs, Editor, Characterization of Catalytic Materials, Butterworths, Stoneham, MA, 1992, pp. 1–16.
[3] I.E. Wachs and K. Segawa, in I.E. Wachs, Editor, Characterization of Catalytic Materials, Butterworths, Stoneham, MA, 1992, pp. 69–88.
[4] R.K. Grasselli and A.W. Sleight, Editors, in Structure–Reactivity and Selectivity Relationships in Heterogeneous Catalysis, Elsevier, Amsterdam, 1991.
[5] T.S. Oyama and J. Hightower, Editors, in Catalytic Selective Oxidation, ACS Symp. Ser., 523, Washington D.C., 1993.
[6] J.M. Stencel, Raman Spectroscopy for Catalysis, van Nostrand Reinhold, New York, 1990.
[7] J.G. Grasselli and B.J. Bulkin, Editors, Analytical Raman Spectroscopy, Wiley, New York, 1991.
[8] I.E. Wachs and F.D. Hardcastle, in Catalysis, Vol. 10, Royal Society of Chemistry, Cambridge, UK, 1993, pp. 102–153.
[9] I.E. Wachs, Catal. Today, 27 (1996) 437.
[10] V.V. Guliants, J.B. Benziger, S. Sundaresan, N. Yao and I.E. Wachs, Catal. Lett., 32 (1995) 379.
[11] G. Deo and I.E. Wachs, J. Catal., 146 (1994) 323.
[12] C.R. Brundle, C.A. Evans and S. Wilson, Editors, in Materials Surface Characterization, 1992.
[13] F. Cavani and F. Trifiro, Chemtech, 24 (1994) 18.
[14] G.J. Hutchings, A. Desmartin-Chomel, R. Oller and J.-C. Volta, Nature, 368 (1994) 41.
[15] G. Centi, Editor, Proc. Vanadyl Pyrophosphate Catalysts, Catal. Today, 16 (1993) 1–154.
[16] G. Deo, I.E. Wachs and J. Haber, Critic. Rev. Surf. Chem., 4 (1994) 141.
[17] G. Went, T.S. Oyama and A.T. Bell, J. Phys. Chem., 94 (1990) 4240.
[18] M.A. Vuurman, A.M. Hirt and I.E. Wachs, J. Phys. Chem., 95 (1991) 9928.
[19] J. Datka, A.M. Turek, J.-M. Jehng and I.E. Wachs, J. Catal., 135 (1992) 186.
[20] G. Deo and I.E. Wachs, J. Catal., 146 (1994) 3335.
[21] G. Ramis, G. Busca and V. Lorenzelli, in C. Mortera, A. Zecchina and G. Costa, Editors, Structure and Reactivity of Surfaces, Elsevier, Amsterdam, 1989, pp. 777–786.
[22] B.M. Weckhuysen, R.A. Schoonheydt and I.E. Wachs, in preparation.